

Transverse Energy-Energy Correlations in Next-to-Leading Order in α_s at the LHC

Ahmed Ali^{*†}

Deutsches Elektronen-Synchrotron DESY, D-22607 Hamburg, Germany

E-mail: ahmed.ali@desy.de

This contribution summarizes the computation of the transverse energy-energy correlation (EEC) and its asymmetry (AEEC) in next-to-leading order (NLO) in α_s in proton-proton collisions at the LHC with the center-of-mass energy $E_{\text{c.m.}} = 7$ TeV [1]. These correlations are shown to be insensitive to the QCD factorization- and the renormalization-scales, structure functions of the proton, and for a judicious choice of the jet-size, also the underlying minimum bias events. Hence they can be used to precisely test QCD in hadron colliders and determine the strong coupling $\alpha_s(M_Z)$. We illustrate these features by showing the $\alpha_s(M_Z)$ -dependence of the transverse EEC and the AEEC in the anticipated range $0.11 \leq \alpha_s(M_Z) \leq 0.13$, comparing it with the attendant theoretical uncertainties.

*36th International Conference on High Energy Physics,
July 4-11, 2012
Melbourne, Australia*

^{*}Speaker.

[†]This work, done in collaboration with F. Barreiro, J. Llorente, and W. Wang, is supported partially by DESY, the Alexander-von-Humboldt Stiftung (Germany), and Fundacion Cajamadrid (Spain).

1. Introduction

Hadron jets are powerful quantitative tools to study Quantum Chromo Dynamics (QCD) in high energy physics. In e^+e^- colliders PETRA, PEP and LEP, and also in the electron-proton collider HERA, jet studies have been undertaken extensively, yielding a consistent and precise value of the QCD coupling constant $\alpha_s(M_Z)$ [2]. At the hadron colliders Tevatron and the LHC, QCD predictions for jets have been compared with the measured transverse momentum (p_T) distributions, and also with the multi-jet rates [3, 4, 5] assuming a jet algorithm [6, 7, 8]. The theoretical framework for calculating the jet cross sections in hadronic collisions in the next-to-leading order (NLO) accuracy has been in place for well over a decade [9, 10], which has been employed in the QCD-based analysis of the hadron collider jet data.

In this paper, we summarize the computation of the transverse energy energy correlation and its asymmetry for pp collisions at the LHC with $\sqrt{s} = 7$ TeV in the NLO accuracy in $\alpha_s(\mu)$, published recently by us [1]. These event shape variables were proposed some time ago [11] as a quantitative measure of perturbative QCD in hadronic collisions. In the leading order in $\alpha_s(\mu)$, these distributions show marked sensitivities on the renormalization and factorization scales $\mu = \mu_R$ and $\mu = \mu_F$, respectively, thereby hindering a determination of $\alpha_s(M_Z)$. This is remedied to a large extent in $O(\alpha_s^2(\mu))$, which reduces the scale-dependence to a few per cent. Hence, there is potential interest in measuring these distributions at the LHC, as they will lead to a quantitative determination of $\alpha_s(M_Z)$ in Terascale hadronic collisions.

In Sec. 2, we give the definitions of the transverse EEC and its asymmetry. In Sec. 3, we present the numerical results calculated in LO and NLO in $\alpha_s(\mu)$ and show that the transverse EEC and its asymmetry in NLO are robust against variations of the various input parameters, including the parton distribution functions (PDFs), and quantify the remaining uncertainties. The sensitivity of these cross sections on $\alpha_s(M_Z)$ is presented in the range $0.11 < \alpha_s(m_Z) < 0.13$ at the LHC ($\sqrt{s} = 7$ TeV).

2. Transverse Energy-Energy Correlation and its asymmetry

The transverse EEC function is defined as: [11]

$$\begin{aligned} \frac{1}{\sigma'} \frac{d\Sigma'}{d\phi} &\equiv \frac{\int_{E_T^{\min}}^{\sqrt{s}} dE_T d^2\Sigma/dE_T d\phi}{\int_{E_T^{\min}}^{\sqrt{s}} dE_T d\sigma/dE_T} \\ &= \frac{1}{N} \sum_{A=1}^N \frac{1}{\Delta\phi} \sum_{\text{pairs in } \Delta\phi} \frac{2E_{Ta}^A E_{Tb}^A}{(E_T^A)^2}, \end{aligned} \quad (2.1)$$

with

$$\sigma' = \int_{E_T^{\min}}^{\sqrt{s}} dE_T d\sigma/dE_T$$

The first sum on the right-hand side in the second of the above equations is over the events A with total transverse energy $E_T^A = \sum_a E_{Ta}^A \geq E_T^{\min}$, with the E_T^{\min} set by the experimental setup. The second sum is over the pairs of partons (a, b) whose transverse momenta have relative azimuthal

angle ϕ to $\phi + \Delta\phi$. In addition, the fiducial volume is restricted by the experimental acceptance in the rapidity variable η .

In leading order QCD, the transverse energy spectrum $d\sigma/dE_T$ is a convolution of the PDFs with the $2 \rightarrow 2$ hard scattering partonic sub-processes. Away from the end-points, i.e., for $\phi \neq 0^\circ$ and $\phi \neq 180^\circ$, the energy-weighted cross section $d^2\Sigma/dE_T d\phi$ involves the convolution of the PDFs with the $2 \rightarrow 3$ sub-processes, such as $gg \rightarrow ggg$. Thus, schematically, the leading contribution for the transverse EEC function is calculated from the following expression:

$$\frac{1}{\sigma'} \frac{d\Sigma'}{d\phi} = \frac{\Sigma_{a_i, b_i} f_{a_1/p}(x_1) f_{a_2/p}(x_2) \star \hat{\Sigma}^{a_1 a_2 \rightarrow b_1 b_2 b_3}}{\Sigma_{a_i, b_i} f_{a_1/p}(x_1) f_{a_2/p}(x_2) \star \hat{\sigma}^{a_1 a_2 \rightarrow b_1 b_2}}, \quad (2.2)$$

where $\hat{\Sigma}^{a_1 a_2 \rightarrow b_1 b_2 b_3}$ is the transverse energy-energy weighted partonic cross section, x_i ($i = 1, 2$) are the fractional longitudinal momenta carried by the partons, $f_{a_1/p}(x_1)$ and $f_{a_2/p}(x_2)$ are the PDFs, and the \star denotes a convolution over the appropriate variables. The function defined in Eq. (2.2) depends not only on ϕ , but also on the ratio E_T^{\min}/\sqrt{s} and rapidity η . The transverse EEC cross section is to a good approximation *independent* of the PDFs [11]. Thus, for a fixed rapidity range $|\eta| < \eta_c$ and the variable E_T/\sqrt{s} , one has an approximate factorized result, which in the LO in $\alpha_s(\mu)$ reads as

$$\frac{1}{\sigma'} \frac{d\Sigma'}{d\phi} \sim \frac{\alpha_s(\mu)}{\pi} F(\phi), \quad (2.3)$$

where

$$\alpha_s(\mu) = \frac{1}{b_0 \log(\mu^2/\Lambda^2)} \left[1 - \frac{b_1 \log(\log(\mu^2/\Lambda^2))}{b_0^2 \log(\mu^2/\Lambda^2)} \right], \quad b_0 = \frac{33 - 12n_f}{12\pi}, \quad b_1 = \frac{153 - 19n_f}{24\pi^2}. \quad (2.4)$$

In the above equation, n_f is the active quark flavor number at the scale μ and the hadronization scale Λ is determined by the input $\alpha_s(m_Z)$. The function $F(\phi)$ and the corresponding transverse EEC asymmetry defined as

$$\frac{1}{\sigma'} \frac{d\Sigma'^{\text{asym}}}{d\phi} \equiv \frac{1}{\sigma'} \frac{d\Sigma'}{d\phi} \Big|_{\phi} - \frac{1}{\sigma'} \frac{d\Sigma'}{d\phi} \Big|_{\pi-\phi}, \quad (2.5)$$

were worked out in [11] in the leading order of $\alpha_s(\mu)$ for the CERN SPS $p\bar{p}$ collider at $\sqrt{s} = 540$ GeV.

3. Next-to-leading order results for the transverse EEC and its asymmetry

In Ref. [1], the program NLOJET++ [10] was used to compute the transverse EEC and its asymmetry AEEC in the NLO accuracy for the LHC proton-proton center-of-mass energy $\sqrt{s} = 7$ TeV. Schematically, this entails the calculations of the $2 \rightarrow 3$ partonic sub-processes in the NLO accuracy and of the $2 \rightarrow 4$ partonic processes in the leading order in $\alpha_s(\mu)$, which contribute to the numerator on the r.h.s. of Eq. (2.2). We have restricted the azimuthal angle range by cutting out regions near $\phi = 0^\circ$ and $\phi = 180^\circ$. This would, in particular, remove the self-correlations ($a = b$) and frees us from calculating the $O(\alpha_s^2)$ (or two-loop) virtual corrections to the $2 \rightarrow 2$ processes. Thus, with the azimuthal angle cut, the numerator in Eq. (2.2) is calculated from the $2 \rightarrow 3$ and

$2 \rightarrow 4$ processes to $O(\alpha_s^4)$. The denominator in Eq. (2.2) includes the $2 \rightarrow 2$ and $2 \rightarrow 3$ processes, which are calculated up to and including the $O(\alpha_s^3)$ corrections.

In the NLO accuracy, one can express the EEC cross section as

$$\frac{1}{\sigma'} \frac{d\Sigma'}{d\phi} \sim \frac{\alpha_s(\mu)}{\pi} F(\phi) \left[1 + \frac{\alpha_s(\mu)}{\pi} G(\phi) \right]. \quad (3.1)$$

It is customary to lump the NLO corrections in a so-called K -factor (which, as shown here, is a non-trivial function of ϕ), defined as

$$K^{\text{EEC}}(\phi) \equiv 1 + \frac{\alpha_s(\mu)}{\pi} G(\phi). \quad (3.2)$$

The transverse EEC asymmetry in the NLO accuracy is likewise defined as

$$\frac{1}{\sigma'} \frac{d\Sigma'^{\text{asym}}}{d\phi} \sim \frac{\alpha_s(\mu)}{\pi} A(\phi) \left[1 + \frac{\alpha_s(\mu)}{\pi} B(\phi) \right]. \quad (3.3)$$

and the corresponding K -factor is defined as

$$K^{\text{AEEC}}(\phi) \equiv 1 + \frac{\alpha_s(\mu)}{\pi} B(\phi). \quad (3.4)$$

The principal result of [1] is the calculation of the NLO functions $K^{\text{EEC}}(\phi)$ and $K^{\text{AEEC}}(\phi)$ and in demonstrating the insensitivity of the EEC and the AEEC functions, calculated to NLO accuracy, to the various intrinsic parametric and the underlying event uncertainties. In transcribing the NLO-JET++ [10] program, the default structure functions therein have been replaced by the state of the art PDFs, representative of which are the MSTW [12] and the CT10 [13] sets. Also, the k_T jet algorithm used in the NLOJET++ for defining the jets was replaced by the *en vogue* anti- k_T jet algorithm [8], in which the distance measures of partons are given by

$$d_{ij} = \min(k_{ti}^{-2}, k_{tj}^{-2}) \frac{(\eta_i - \eta_j)^2 + (\phi_i - \phi_j)^2}{R^2}, \quad d_{iB} = k_{ti}^{-2}, \quad (3.5)$$

with R being the usual radius parameter. We have assumed the rapidity range $|\eta| \leq 2.5$, have put a cut on the transverse energy $E_T > 25$ GeV for each jet and require $E_{T1} + E_{T2} > 500$ GeV for the two leading jets. The latter cut ensures that the trigger efficiencies for the LHC detectors will be close to 100%. We have set the transverse energy of the hardest jet as the default factorization- and renormalization-scale, i.e., $\mu_F = \mu_R = E_T^{\text{max}}$. We then vary the scales μ_F and μ_R independently in the range $0.5 E_T^{\text{max}} \leq (\mu_F, \mu_R) \leq 2 E_T^{\text{max}}$ to study numerically the scale dependence. The effects induced by the underlying event, multiparton interactions and hadronization effects have been studied in [1] using the PYTHIA6 MC [14]. They were computed for two representative values $R=0.6$ and $R=0.4$. These effects were found to be small. Typically, the effect of hadronization on the transverse EEC is found to be $\leq 5\%$ and from the underlying event $\leq 6\%$ for the jet-size parameter $R = 0.6$. The corresponding numbers are $\leq 5\%$ and $\leq 2\%$ for $R = 0.4$. To reduce the effect of the parton showers in the transverse EEC and the AEEC distributions, $\cos \phi$ is restricted to the range $[-0.8, 0.8]$.

The dependence of the transverse EEC calculated in the NLO accuracy on the PDFs is shown in Fig. 1 for the two widely used sets: MSTW [12] and CT10 [13], using their respective central

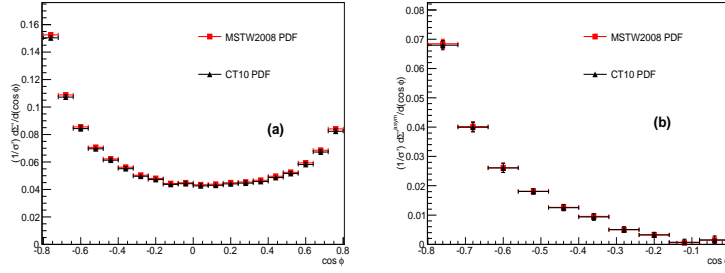


Figure 1: (color online) Dependence of the transverse EEC cross section (a) and its asymmetry (b) on the PDFs at NLO in α_s . Red entries correspond to the MSTW [12] PDFs and the black ones are calculated using the CT10 PDF set [13]. The errors shown reflect the intrinsic parametric uncertainties in each PDF set and the Monte Carlo integration uncertainties.

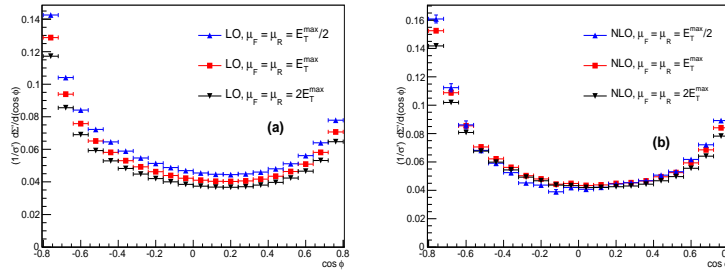


Figure 2: (color online) Dependence of the transverse EEC on the scales μ_F , and μ_R in LO (a) and in the NLO (b) in α_s for the indicated values of the scales, obtained by setting $\mu_F = \mu_R$ and varying it $\mu_F = \mu_R = [0.5, 2] \times E_T^{\max}$.

(default) parameters. This figure shows that the PDF-related differences on the transverse EEC are negligible, with the largest difference found in some bins amounting to 3%, (but typically they are $< 1\%$). The insensitivity of the transverse EEC cross section to the PDFs provides a direct test of the underlying partonic hard processes. In what follows, we will adopt the MSTW [12] PDF set as it provides a correlated range of $\alpha_s(M_Z)$ and the structure functions for the current range of interest for $\alpha_s(M_Z)$: $0.11 < \alpha_s(M_Z) < 0.13$.

We next show the dependence of the transverse EEC cross section and its asymmetry on the factorization and the renormalization scales in the range $(\mu_F, \mu_R) = [0.5, 2] \times E_T^{\max}$ and display them in Fig. 2 for the transverse EEC and in Fig. 3 for the asymmetric transverse EEC. Effects of the variations in the scales μ_F and μ_R on the transverse EEC cross section in the LO are shown in Fig. 2 (a), which is obtained by setting the scales $\mu_F = \mu_R$. The corresponding asymmetry of the transverse EEC cross sections is displayed in Fig. 3 (a). We note that the dominant scale dependence in the LO arises from the variation of the renormalization scale μ_R . The results obtained in the NLO are shown in Fig.2 (b) for the transverse EEC and in Fig. 3 (b) for the asymmetry. One observes significantly less dependence on the scales; in particular the marked μ_R -dependence in the LO is now reduced. Typical scale-variance on the transverse EEC distribution in the NLO is

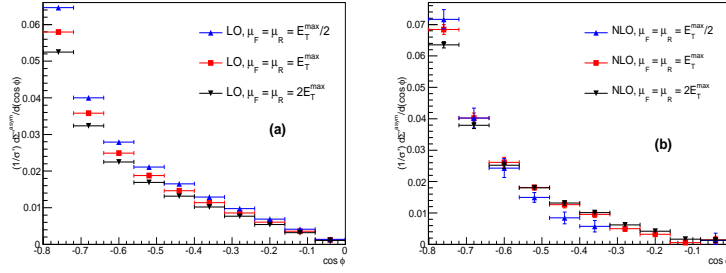


Figure 3: (color online) Same as Fig. 2 but for the asymmetric transverse EEC.

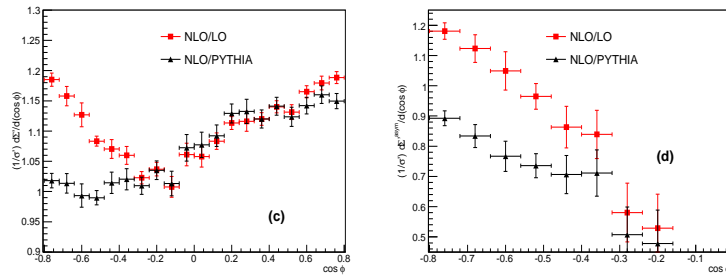


Figure 4: (color online) Comparison of the LO-, NLO-, and the PYTHIA-based results for the transverse EEC and its asymmetry. Left frame displays the function $K^{\text{EEC}}(\phi)$ (boxes, red entries) as defined in Eq. (3.2) and a phenomenological function obtained by replacing the LO results by the PYTHIA MC results (triangles, black entries). Right frame shows the corresponding function $K^{\text{AEEC}}(\phi)$ for the transverse EEC asymmetry defined in Eq. (3.4). The errors shown are described in text.

found to be 2% - 3%, with the largest effects in some bins reaching 5%. This scale-insensitivity in the NLO accuracy is crucial to undertake a quantitative determination of α_s from the collider jet data.

Having shown that the uncertainties due to underlying events and the PDFs are negligible, and the scale dependence is much reduced in the NLO, we present our results for the transverse EEC in the LO and the NLO accuracy and the corresponding results for the transverse AEEC. We also compute these distributions from a MC-based model which has the LO matrix elements and multiparton showers encoded. To be specific, we have used the PYTHIA8 [14] MC program and have generated the transverse EEC and the AEEC distributions. This comparison provides a practically convenient way to correct the PYTHIA8 MC-based theoretical distributions, often used in the analysis of the hadron collider data, due to the NLO effects. In Fig. 4 (left frame), we show the function $K^{\text{EEC}}(\phi)$ defined in Eq. (3.2), and another phenomenological function in which the NLO transverse EEC distribution is normalized to the one generated by the PYTHIA8 [14] MC program. The corresponding function $K^{\text{AEEC}}(\phi)$, defined in Eq. (3.4), is shown in Fig. 4 (right frame). Here also we show the corresponding phenomenological function in which the transverse EEC obtained in NLO is normalized to the ones generated by the PYTHIA MC. The effects of the NLO corrections are discernible, both compared to the LO and PYTHIA8 [14], and they are signif-

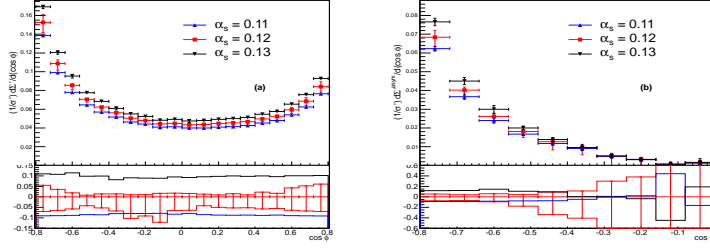


Figure 5: (color online) Transverse EEC cross section (a) and its asymmetry (b) with three values of $\alpha_s(M_Z) = 0.11$ (blue; triangles), $= 0.12$ (red, boxes), and $= 0.13$ (black, inverted triangles). The bottom panel of the figures demonstrate the size of errors (red, histograms with vertical lines) and deviations with the values of $\alpha_s(M_Z) = 0.11$ (blue, lower histogram) and $= 0.13$ (black, upper histogram) from the results evaluated with $\alpha_s = 0.12$.

icant in the large-angle region (i.e., for $\cos \phi < 0$). Thus, the NLO effects in the EEC distribution reduce the scale-dependence, in particular on μ_R , and distort the shape of both the EEC and AEEC distributions, providing a non-trivial test of the NLO effects.

We now discuss the main interest in this work, which is the sensitivity of the transverse EEC and the AEEC on $\alpha_s(M_Z)$. In relating the strong coupling $\alpha_s(\mu)$ at a certain scale relevant for the collider jets, such as $\mu = E_T^{\max}$, to the benchmark value $\alpha_s(M_Z)$, we have used the two-loop β -function and the explicit formula for transcribing $\alpha_s(\mu)$ to $\alpha_s(M_Z)$ can be seen in Eq. (2.4). Results for the transverse EEC and the AEEC are shown in Fig. 5 (a) and Fig. 5 (b), respectively, for the three indicated values of $\alpha_s(M_Z) = 0.11$ (blue; triangles), $= 0.12$ (red, boxes), and $= 0.13$ (black, inverted triangles). The scale uncertainties are included only in the curve corresponding to $\alpha_s(M_Z) = 0.12$, as it is close to the current world average $\alpha_s(M_Z) = 0.1184$ [16] and hence our focus on this value. To demonstrate the intrinsic errors in the calculations of the transverse EEC and its asymmetry, we show the percentage size of the errors in the lower part of Fig. 5 (a) and Fig. 5 (b), respectively, for $\alpha_s(M_Z) = 0.12$. Concentrating first on the transverse EEC, we see that the bin-by-bin errors are typically $+2\%$ and -6% (for $|\cos \phi| \leq 0.6$), and somewhat larger for $|\cos \phi| > 0.6$. A part of this error is of statistical origin in our Monte Carlo based theoretical calculations and is reducible, in principle, with the help of a more effective importance sampling algorithm in the event generation. However, a part of the error is irreducible, given the current theoretical (NLO) precision. This is quantified for the normalized integrated transverse EEC X-section over the $\cos \phi$ range shown in the figures above, which largely removes the statistical (bin-by-bin) error:

$$\frac{\alpha_s(m_Z)}{\langle \frac{1}{\sigma'} \frac{d\Sigma'}{d\phi} \rangle} \begin{array}{|c|c|c|} \hline 0.11 & 0.12 & 0.13 \\ \hline 0.092^{+0.001}_{-0.005} & 0.101^{+0.001}_{-0.005} & 0.111^{+0.001}_{-0.005} \\ \hline \end{array} \quad (3.6)$$

The computational error on the transverse AEEC is larger, as shown in Fig. 5 (b) for $\alpha_s(M_Z) = 0.12$. In particular, the errors for the last four bins in the AEEC X-section are large due to the intrinsically small value of this cross-section as $\cos \phi \rightarrow 0$. However, in the region $-0.8 \leq \cos \phi \leq -0.4$, a clear dependence of the differential transverse AEEC on $\alpha_s(M_Z)$ is discernible. This is also displayed for the normalized integrated transverse AEEC X-section given below (in units of 10^{-3}),

in which the last four bins contribute very little:

$$\frac{\alpha_s(m_Z)}{\langle \frac{1}{\sigma'} \frac{d\Sigma'^{asymm}}{d\phi} \rangle} \left| \begin{array}{c|c|c} 0.11 & 0.12 & 0.13 \\ \hline 13.6^{+0.2}_{-1.4} & 14.8^{+0.3}_{-1.5} & 16.4^{+0.4}_{-1.6} \end{array} \right. \quad (3.7)$$

4. Summary

We have summarized the LO and the NLO results for the transverse EEC and its asymmetry for jets at the LHC computed in [1]. These distributions are shown to have all the properties that are required for the precision tests of perturbative QCD. In particular, they (i) are almost independent of the structure functions, with typical uncertainties at 1%, (ii) show weak scale sensitivity; varying the scale from $\mu = E_T/2$ to $\mu = 2E_T$, the uncertainties are less than 5% with the current (NLO) theoretical accuracy, (iii) their dependence on modeling the underlying minimum bias events for judicious choice of the parameter R is likewise mild, ranging typically from 2% to 5% as one varies from $R = 0.4$ to $R = 0.6$, and (iv) preserve sensitivity to $\alpha_s(M_Z)$; varying $\alpha_s(M_Z) = 0.11$ to 0.13 , the transverse EEC (AEEC) cross section changes approximately by 20% (15%), and thus these distributions will prove to be powerful techniques for the quantitative study of event shape variables and in the measurement of $\alpha_s(M_Z)$ in hadron colliders.

References

- [1] A. Ali, F. Barreiro, J. Llorente and W. Wang, Phys. Rev. D **86**, 114017 (2012) [arXiv:1205.1689 [hep-ph]].
- [2] K. Nakamura *et al.* [Particle Data Group], J. Phys. G **37**, 075021 (2010).
- [3] For a review of recent QCD results from the Tevatron, see, for example, M. Wobisch, Nucl. Phys. B Proc. Suppl. (2012) (in press) and arXiv:1202.0205 [hep-ex].
- [4] S. Chatrchyan *et al.* [CMS Collaboration], arXiv:1204.0696 [hep-ex].
- [5] G. Aad *et al.* [Atlas Collaboration], Eur. Phys. J. C **71**, 1512 (2011) [arXiv:1009.5908 [hep-ex]].
- [6] S. Catani, Y. L. Dokshitzer, M. H. Seymour and B. R. Webber, Nucl. Phys. B **406**, 187 (1993).
- [7] S. Catani and M. H. Seymour, Nucl. Phys. B **485**, 291 (1997) [Erratum-ibid. B **510**, 503 (1998)]; [arXiv:hep-ph/9605323].
- [8] M. Cacciari, G. P. Salam and G. Soyez, JHEP **0804**, 063 (2008) [arXiv:0802.1189 [hep-ph]].
- [9] S. Catani and M. H. Seymour, Phys. Lett. B **378**, 287 (1996) [arXiv:hep-ph/9602277].
- [10] Z. Nagy, Phys. Rev. Lett. **88**, 122003 (2002) [arXiv:hep-ph/0110315]; Phys. Rev. D **68**, 094002 (2003) [arXiv:hep-ph/0307268].
- [11] A. Ali, E. Pietarinen and W. J. Stirling, Phys. Lett. B **141**, 447 (1984).
- [12] A. D. Martin, W. J. Stirling, R. S. Thorne and G. Watt, Eur. Phys. J. C **63**, 189 (2009).
- [13] H. L. Lai *et al.*, Phys. Rev. D **82**, 074024 (2010).
- [14] T. Sjostrand, S. Mrenna and P. Z. Skands, Comput. Phys. Commun. **178**, 852 (2008) [arXiv:0710.3820 [hep-ph]].
- [15] M. Bahr *et al.*, Eur. Phys. J. C **58**, 639 (2008) [arXiv:0803.0883 [hep-ph]]; arXiv:1102.1672[hep-ph]].
- [16] J. Beringer *et al.* [Particle Data Group Collaboration], Phys. Rev. D **86**, 010001 (2012).